Georgia Tech Sponsored Research

14

Project	E-20-F75
Project director	JACOBS LAURENCE
Research unit	CEE
Title	GAS TURBINE ENGINE PROGNOSTICS AND EQUIPMENT HEALTH MANAGEMENT
Project date	8/31/2001

MEMS Sensors for the Non-Contact Ultrasonic Monitoring of Gas Turbine Engine Components during High-Temperature Testing

First Year Report, August 31, 2001

Principal Investigators:
F. Levent Degertekin Assistant Professor of Mechanical Engineering.
Jacek Jarzynski Professor of Mechanical Engineering
Laurence J. Jacobs Professor of Civil and Environmental Engineering

Graduate Research Assistant:
Matt Abercrombie

Research Objective:
The objective of this project is to design, assemble and test miniature acoustic sensors for high-temperature condition monitoring of gas turbine engine components. These microphones can be used for either passive monitoring of the acoustic signals within the engine's hot gas stream, or the same technology can be extended to develop air-coupled transmitting transducers needed for in-service, active ultrasonic evaluation methodologies. These sensors enable the *in situ* measurement of acoustic signals that can be used in a quantitative, prognostic model to predict an in-service gas turbine engine component's remaining life.

Benefits to GEPS:
These MEMS sensors will enable robust, in situ acoustic measurements through higher temperatures and a broader frequency bandwidth than currently possible. A dynamic pressure testing facility is being used to develop a benchmark calibration procedure for acoustic sensors and to characterize the effect of sensor performance and mounting.

MEMS Sensor Development:
Optical probe setup and demonstration of pressure sensitivity
The acoustic MEMS sensor to be developed in this project is shown schematically in Fig. 1. It consists of a surface micromachined reflecting membrane and a diffraction grating built on an optically transparent substrate. The gap between the membrane and the grating is vacuum-sealed so that any external pressure will deflect the membrane. This deflection is measured by illuminating the diffraction grating from the backside through the transparent substrate, and monitoring the intensity of the reflected diffraction orders.

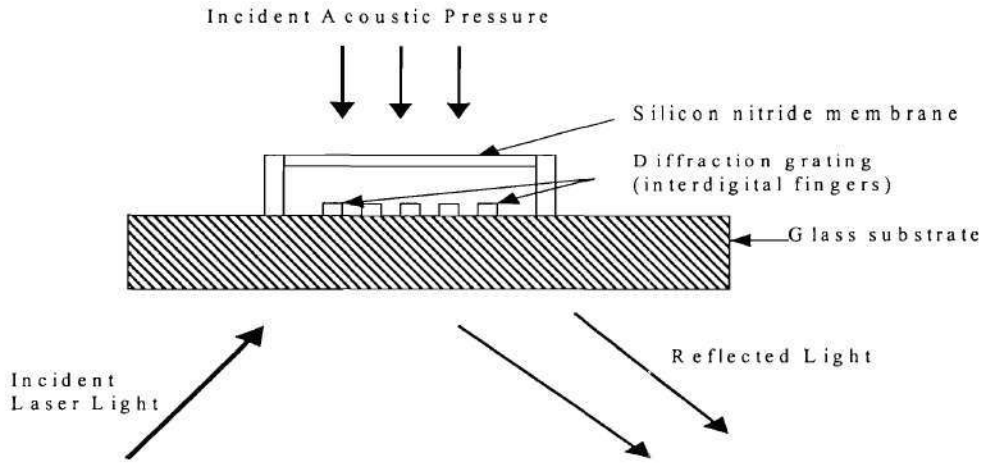

Figure 1. Schematic of the MEMS acoustic pressure sensor based on phase sensitive optical diffraction grating.

A low temperature version of the MEMS sensor, which is essentially a broadband microphone, has been built using aluminum membrane and diffraction fingers on quartz and tested using the setup shown in Fig. 2. The photograph of the optical probe setup is also shown in Fig. 3. It consists of a 4mW HeNe laser focused down to a 20μm spot on a desired diffraction grating under the MEMS sensor membrane. The reflected field consists of the direct reflection (0^{th} order) and the higher diffraction orders as seen in Fig. 3. The first diffraction order intensity is monitored using a photodetector to measure the deflection of the membrane.

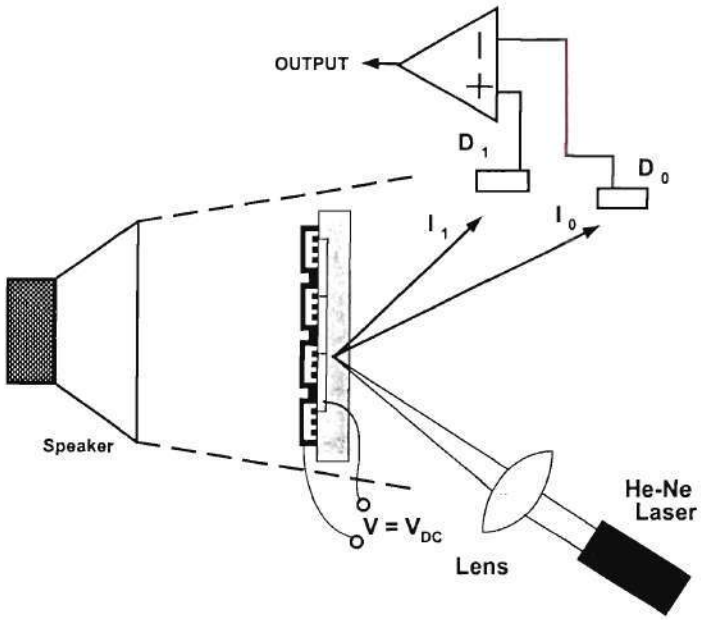

Figure 2. Schematic of the setup implemented for measurement and characterization of the MEMS sensor at atmospheric pressure and room temperature.

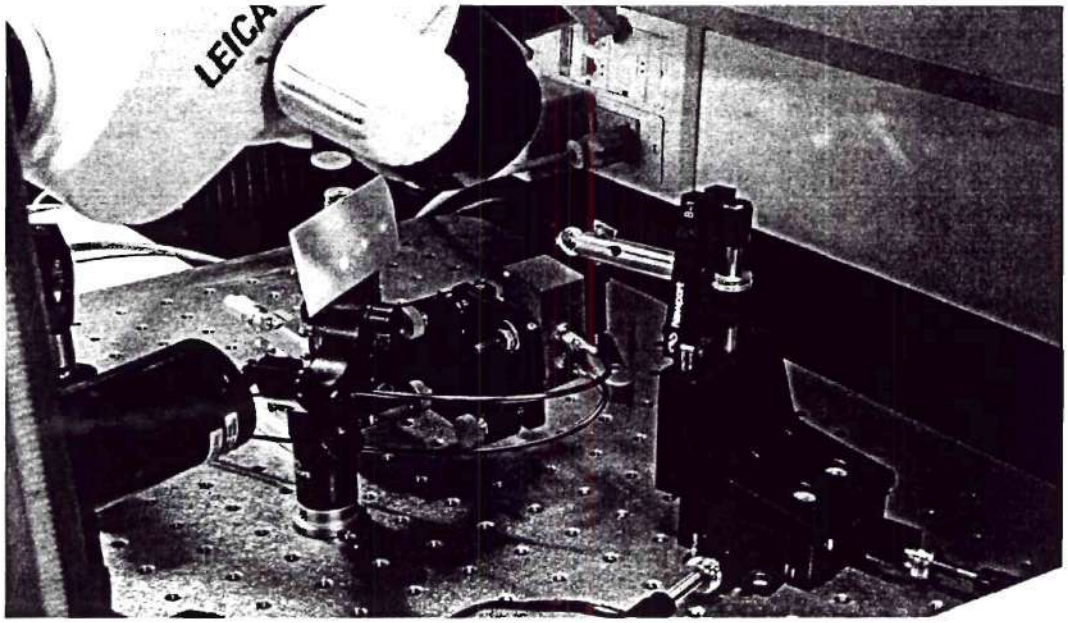

Figure 3. Photograph of the setup in Fig. 2 showing the laser and the reflected diffraction orders projected on a piece of paper.

In this particular case with aluminum membrane and diffraction fingers it is also possible to apply electrostatic actuation forces to trace the sensitivity curve for the MEMS sensor as shown in Fig. 4-A. To measure the pressure sensitivity of the sensor, a speaker is used as the external pressure source as shown in Fig. 2 and the pressure field generated by this speaker is measured using a sound meter. As a sample signal, 5 cycles of a sine wave at 20kHz is applied to the speaker generating 80dB SPL (0.2Pa-rms) pressure at the sensor surface. Figure 4-B shows the received signal at the detector output at different DC bias levels, showing the effect of quiescent membrane position on sensitivity. In accordance with Fig. 4-A, once can adjust the sensitivity and polarity of the output signal. The signal to noise measurements show that the MEMS sensor structure can measure 0.02Pa level pressure with 20kHz bandwidth. The corresponding displacement sensitivity is around 1x10-4 Å/√Hz, showing the optical interferometric sensitivity achieved by this simple structure.

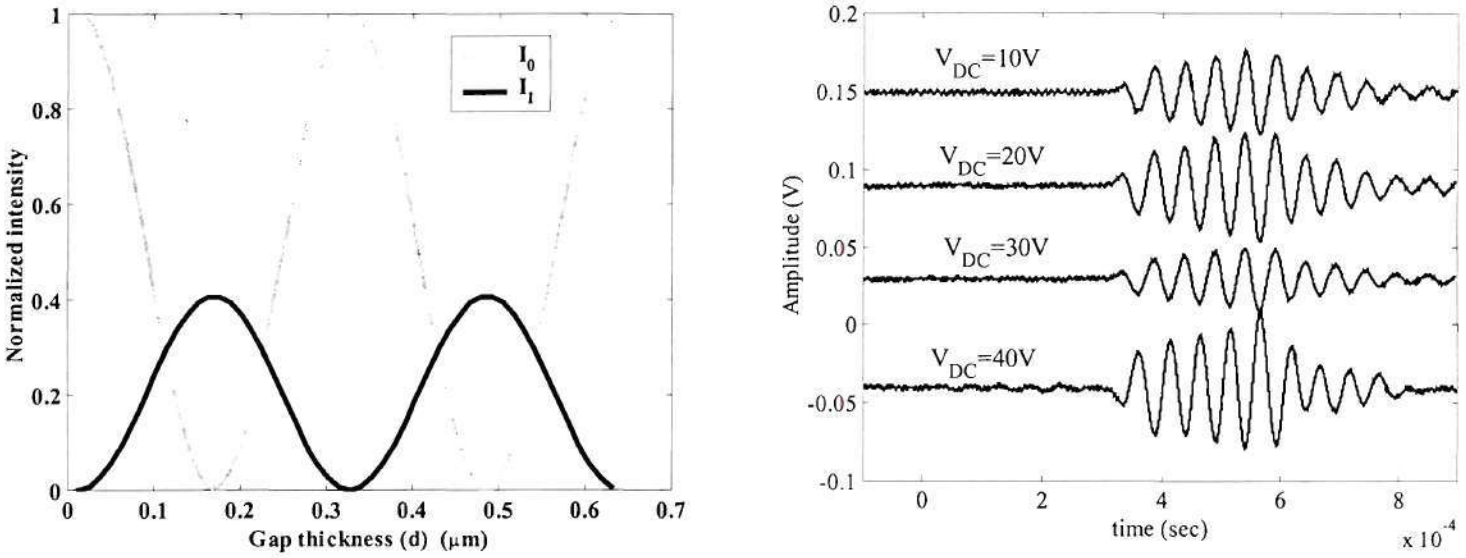

A B

Figure 4. A) Variation of diffracted order intensities as a function of membrane-substrate gap thickness. B) Received optical signals in response to the transient pressure waves generated by the speaker at 20kHz.

Finite Element Modeling of the Acoustic Sensor

In order to predict the acoustic pressure measurement performance of the acoustic sensor and its survivability at high temperature and pressure, the finite element method (FEM) is used. The commercially available FEM program ANSYS is employed for the analysis and the results are compared with analytical results for sample cases such as fully clamped circular plates. The FEM analysis involved a) the static deflection of the membrane under high static pressure, b) static deflection of the membrane due to thermal expansion mismatch between the membrane and substrate at elevated temperatures, c) maximum stress developed in the membrane material, d) dynamic response of the pre-

stressed membrane at high static pressures. The FEM analysis provided important insight into the design of the sensor such as the membrane thickness and diameter required for pressure sensitivity, the gap thickness to prevent collapse at high pressure and temperature and verification of material selection.

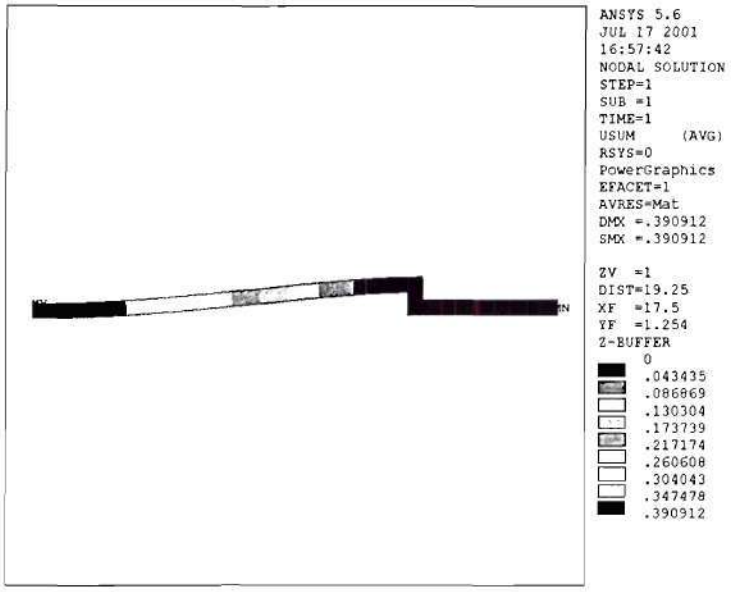

Figure 5. Deflection profile of the silicon nitride MEMS sensor membrane under static pressure. The membrane has a thickness of 1μm, diameter of 50μm and separated from the substrate by 1.5μm gap.

The FEM proved especially useful in revealing some unexpected characteristics of the anchored structure sensor membrane. Figure 5 shows the axi-symmetric model of the of the circular membrane and its deflection with 15Atm ambient pressure. The membrane is made of silicon nitride and has a diameter of 50μm and a thickness of 1μm. In this particular case, the gap thickness is chosen to be 1.5μm, which is relevant to the static deflection due to the anchored structure. A plot of the maximum membrane deflection as a function of ambient pressure is then obtained by changing the static pressure level. The results are plotted in Fig. 6, which shows that the maximum deflection will be around 0.65μm at 25Atm level hence showing that the sensor membrane will not collapse under typical operating pressure.

The effect of temperature on the membrane structure is modeled using the thermal stress module of the FEM software package. The thermal expansion coefficients for silicon nitride and sapphire are obtained from literature and the difference in these coefficients is assumed to generate the thermal stress in the membrane structure. The temperature is varied from 800°C down to 23°C, since the silicon nitride membrane is deposited on the sapphire wafer at around 800°C. Since the thermal expansion coefficient of sapphire is larger than silicon nitride, the membrane experiences compressive stress when the temperature is decreased. The FEM shows that the anchored membrane will definitely buckle up in this case as opposed to an equal probability of buckling up or down in case

of a fully clamped membrane. This is advantageous for the sensor showing that the sensor membrane will not collapse assuming that it has not been collapsed during the initial fabrication stage.

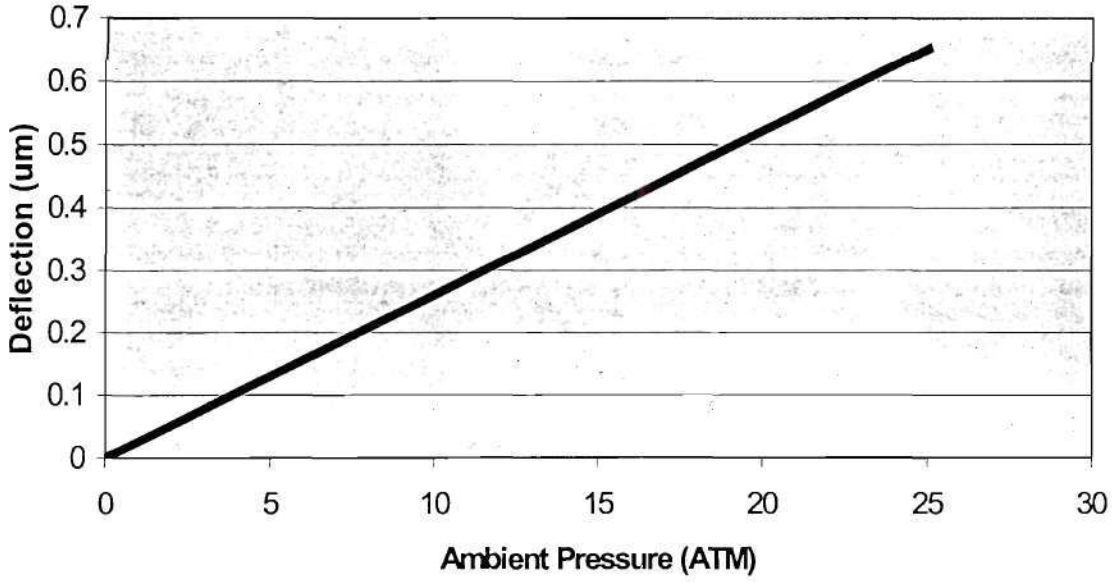

Figure 6. Maximum calculated deflection of the membrane as a function of ambient pressure level.

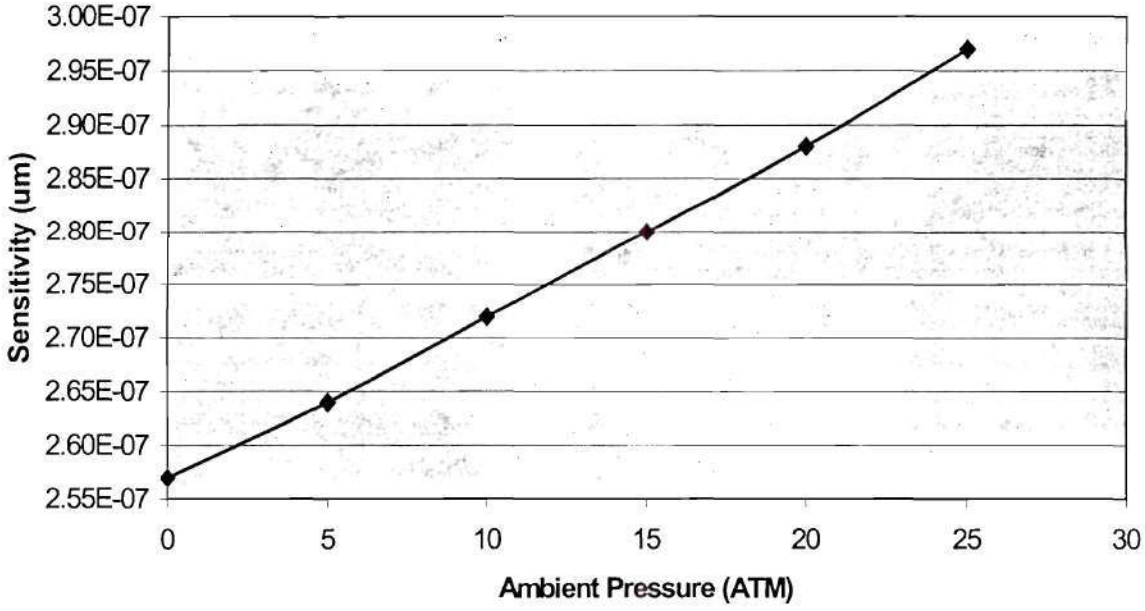

Figure 7. Deflection of the MEMS sensor membrane with 1Pa pressure at 5kHz as a function of ambient pressure. The vertical scale is in micrometers.

The dynamic response of the sensor membrane is also modeled to determine the mechanical sensitivity and bandwidth of the acoustic sensor. The effect of high ambient pressure is taken into account by first applying the static pressure to find the static stress on the structure and then performing time harmonic analysis at 5kHz with 1Pa pressure excitation while the structure is kept under the static stress. The results of this analysis is shown in Fig. 7, which indicates that the mechanical sensitivity of the membrane will be 2.55×10^{-3} Å/Pa at atmospheric pressure and will increase to 2.95×10^{-3} Å/Pa at 25Atm. This behavior is expected since the static pressure bends the membrane rather than stretching it due to the anchored membrane structure. Assuming that the optical detection scheme has a noise level of 1×10^{-4} Å$\sqrt{\text{Hz}}$, the MEMS sensor should be able to detect pressures as low as 10Pa with 40kHz bandwidth.

The variation of the bandwidth of the MEMS sensor with static pressure is also modeled using the FEM. In this case, a modal analysis of the structure is carried out to track the lowest order resonance frequency of the sensor membrane. The results are shown in Fig. 8 for the silicon nitride membrane with the same dimensions as in Fig. 5. The resonance frequency of the sensor membrane is around 7MHz and decreases with increasing static pressure in accordance with the mechanical sensitivity. Assuming that the sensor response will be essentially constant below 80% of the resonance frequency, the MEMS sensor will have a flat frequency response in the DC-5MHz range with high pressure sensitivity as mentioned above.

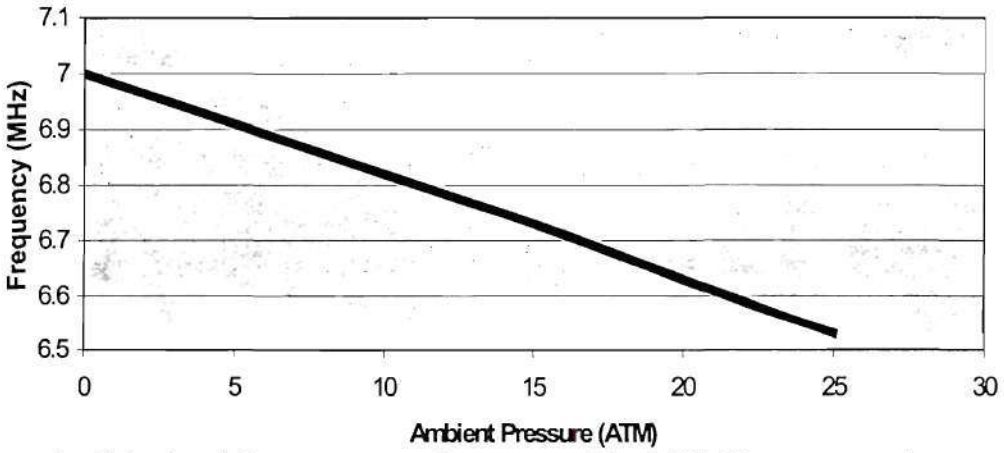

Figure 8. Calculated first resonance frequency of the MEMS sensor membrane as a function of ambient pressure.

MEMS Sensor Process Development

The manufacturing process for the MEMS sensor involved several steps including lithographic mask design and fabrication, process development for high temperature low-pressure deposition of thin films using the CMOS compatible furnace facilities at MiRC, and actual fabrication of the devices. So far, the process development and mask design phases are completed and the fabrication of the final design is currently in progress.

Process Flow

The process flow for the MEMS sensor is shown schematically in Fig. 9. The structure is essentially the same as the low temperature microphone with the exception of high temperature materials and vacuum-sealed membranes. The substrate is chosen as 0.5mm thick double side polished sapphire wafer due to its stability at high temperatures and mechanical strength in addition to being optically transparent. The membrane material is silicon nitride, which is deposited using the Low Pressure Chemical Vapor Deposition (LPCVD) method at 800°C. The tensile stress in this film is controlled by the amount of silicon content, which in turn is determined by the flow rate ratio of DCS and ammonia. The diffraction fingers are made of polysilicon, which is deposited around 600°C and can be made conductive by a subsequent doping process. For the passive MEMS sensor conductivity is not important and the optical properties of polysilicon is not affected significantly by doping. Hence in the first fabrication run, undoped polysilicon is used to form the diffraction grating.

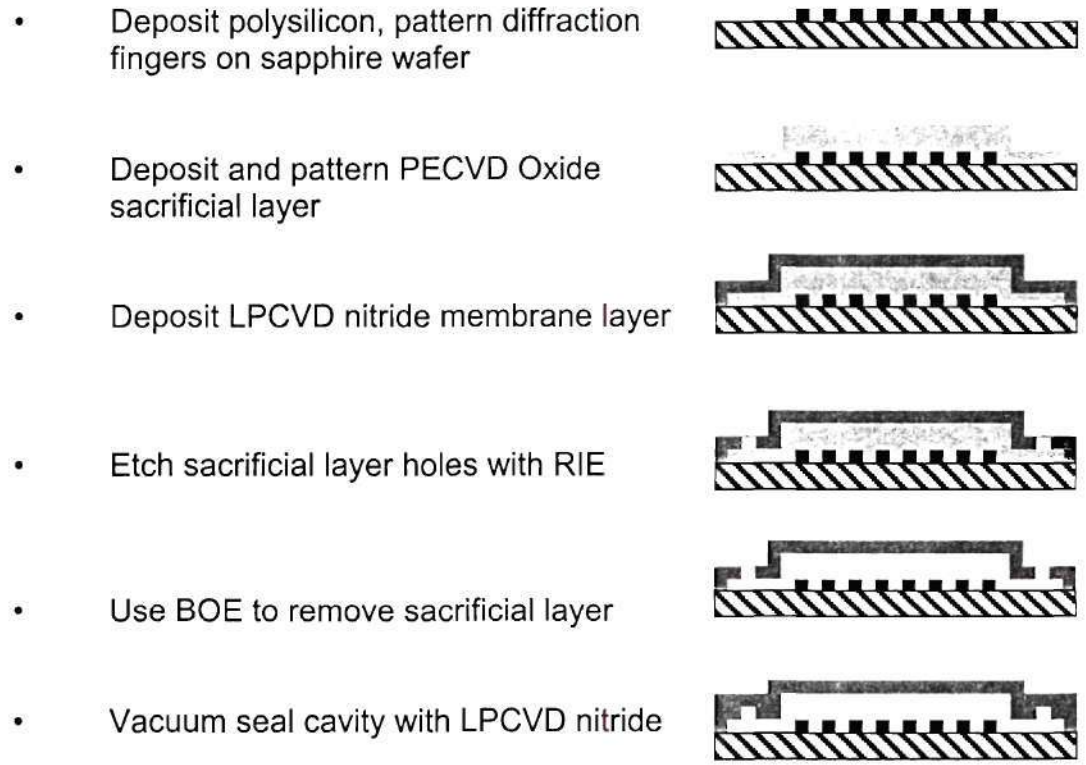

Figure 9. Process flow schematic for the high temperature acoustic MEMS sensor.

As the sacrificial layer, silicon oxide film is used due to the constraints of CMOS furnaces. Plasma Enhanced Chemical Vapor Deposition (PECVD) method is used to deposit for 1.5μm thick silicon oxide layer and buffered oxide etch is used to remove the sacrificial layer after silicon nitride membrane deposition.

Mask Design

One of the advantages of MEMS technology is the ability to fabricate many identical devices in parallel. In a research project, this allows one to try different device configurations to optimize a design. Although the finite element method is used extensively to determine the mechanical structure for the MEMS sensor, many variations in the two dimensions of the MEMS sensor were included in the photolithographic masks. The third dimension, namely the thickness of the deposited films, is controlled by the deposition or etching process time. In addition to different membrane and diffraction grating sizes, sensors with active structures are also considered and contact pads are connected to the diffractive fingers for electrostatic actuation in some MEMS sensors. The process flow shown in Fig. 9 requires 6 masks including an extra mask to etch down the membrane to the desired thickness after the vacuum-sealing step. These mask details are shown in Fig. 10 along with the overall mask pattern for the first polysilicon layer.

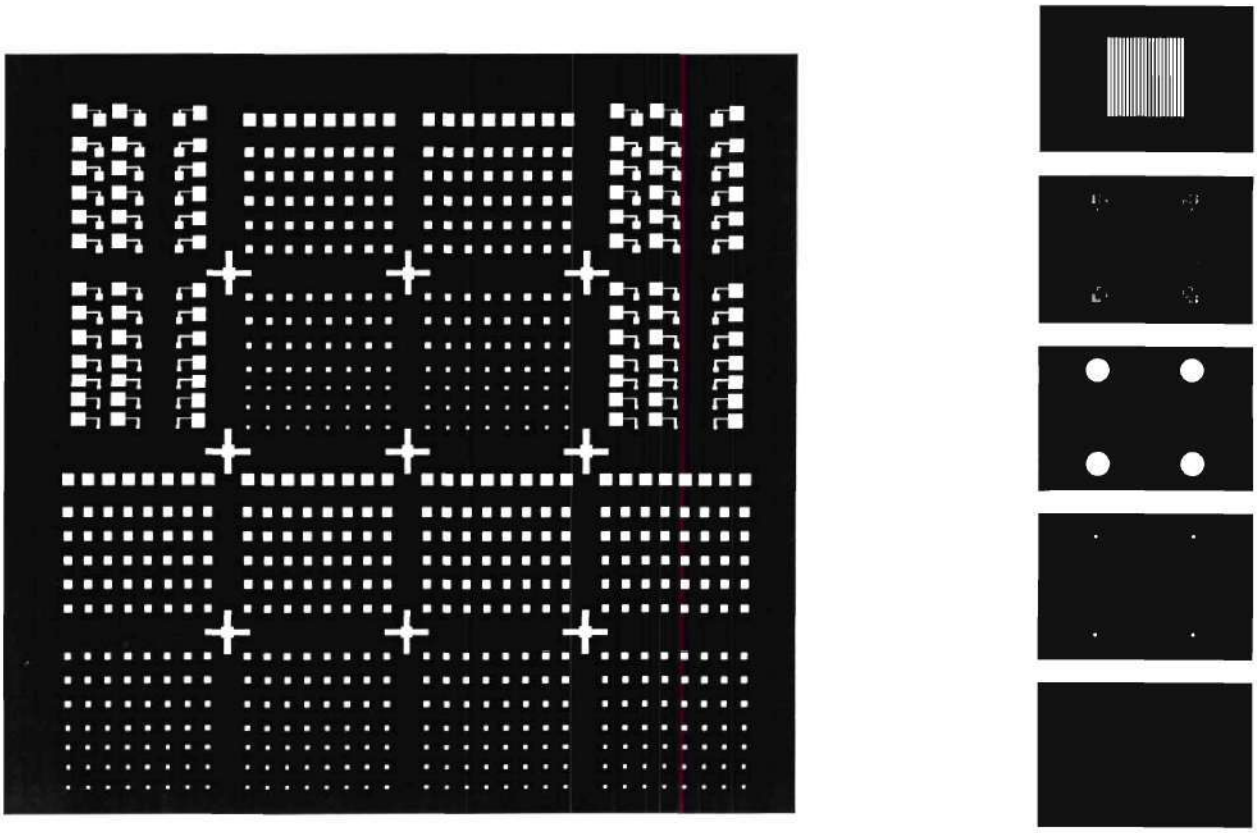

Figure 10. The repeated mask pattern (left) and the details of the masks used during the process steps shown in Fig. 9.

Figure 10 shows the overall mask layout which have the following varieties: a) Membrane diameter: 40-200μm, b) Membrane shape: Circle, octagon, hexagon, c) Diffraction grating period: 1.5-3μm, d) Electrically active and passive. This wide variation allows for process optimization and characterization many MEMS devices with wide dynamic range and testing the dependence of mechanical sensitivity on geometrical parameters. The actual size of the mask shown in Fig. 10 is 9x9mm and 25 copies of this pattern are fitted on a single sapphire wafer.

Process Development and Device Fabrication

One of the major tasks in this project is the development of the fabrication procedures for the MEMS sensor. This proved to be quite a challenge due to several reasons. The furnaces in the Microelectronics Research Center (MiRC) are predominantly used for LPCVD of silicon nitride and polysilicon deposition for CMOS circuit fabrication. Hence, these furnaces had been exclusively used for silicon processing. Introducing a non-silicon substrate required a series of CMOS test runs for ion contamination and implementation of a separate RCA cleaning line for sapphire wafers. Since the MiRC is a multi-user university facility, the systems are down more frequently as compared to an industrial fab. Despite these impeding factors, all the process steps required in the process flow shown in Fig. 8have been developed and tested on sapphire wafers.

The fabrication of the actual high temperature MEMS sensor has started and several steps shown in Fig. 9 are implemented. Fig. 11 shows the deposited and patterned polysilicon diffraction fingers on sapphire which are connected to a contact pad for electrostatic actuation. The polysilicon layer is 0.24μm thick, and initial optical tests show that this layer is suitable to build an efficient diffraction grating on sapphire substrates.

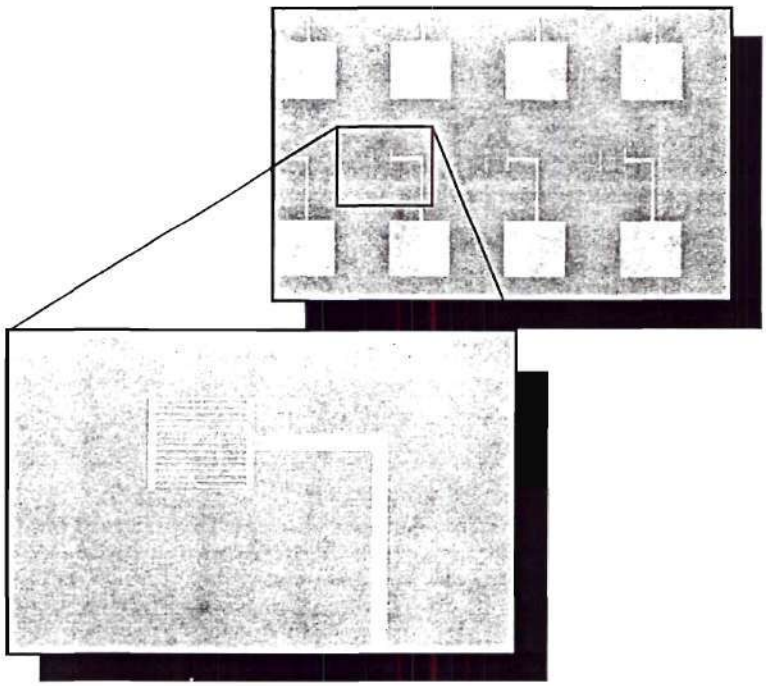

Figure 11. The view of a section of the patterned polysilicon layer and a detailed view of a diffraction grating built on sapphire substrate. These particular sensors will be electrically active is desired. The large square regions are for electrical contact pads.

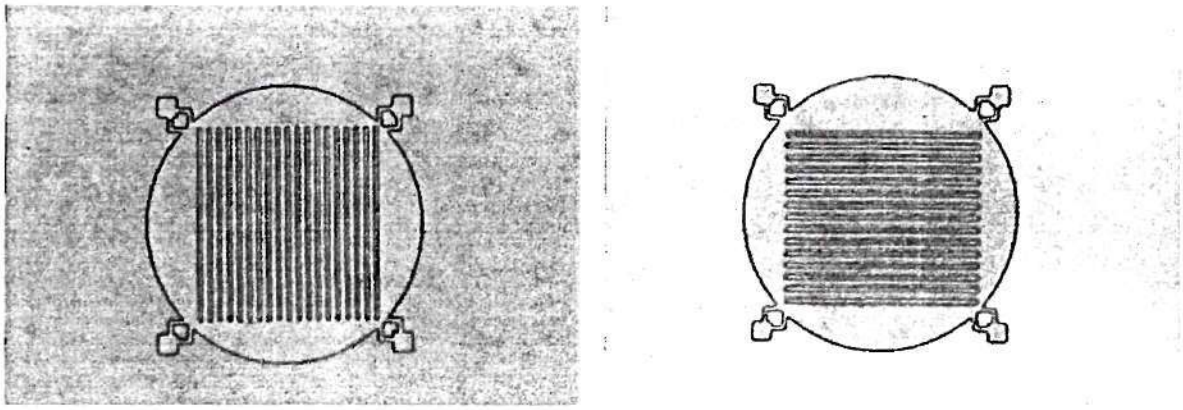

Figure 12. Optical micrograph of a MEMS sensor membrane with diffraction grating during the sacrificial layer patterning process in PECVD chamber. Left: Before patterning, membrane region covered by photoresist, Right: After patterning to define the sensor membrane.

Figure 12 shows another wafer at a later stage of device fabrication (step 2 in Fig. 9) which determines the lateral size of the MEMS sensor membrane. The membrane has 100μm diameter and the diffraction grating has a period of 4μm. The thin linear structure at the four corners are the etch channels from which BOE solution will enter and dissolve the oxide layer during the sacrificial layer etch step. The picture on the left shows the resist pattern on the sacrificial silicon oxide layer before patterning. The picture on the right is taken after the sacrificial layer patterning step in PECVD etch station. This particular device will be electrically passive, as the diffraction fingers are not connected to any electrical contact pad. The device fabrication is currently in progress and it is estimated that fully functional devices will be ready for testing in the next 4 months.

Dynamic Pressure Measurements:

This portion of the project developed a benchmark, test-bed to calibrate the performance of acoustic sensors in gas turbine engines. This test-bed includes a horn system to create a controlled, high-pressure acoustic signal, an oven for high temperature testing (including sensor durability and high temperature performance) and the development of a calibration procedure. A schematic of the horn system is shown in Fig. 13.

An example of the horn's calibration capability is shown in the Fig.14, which shows the response of a commercial Endevco sensor, plus the transfer function for two different holder designs. This figure demonstrates the type of calibration measurements that can be made in the pressure test-bed.

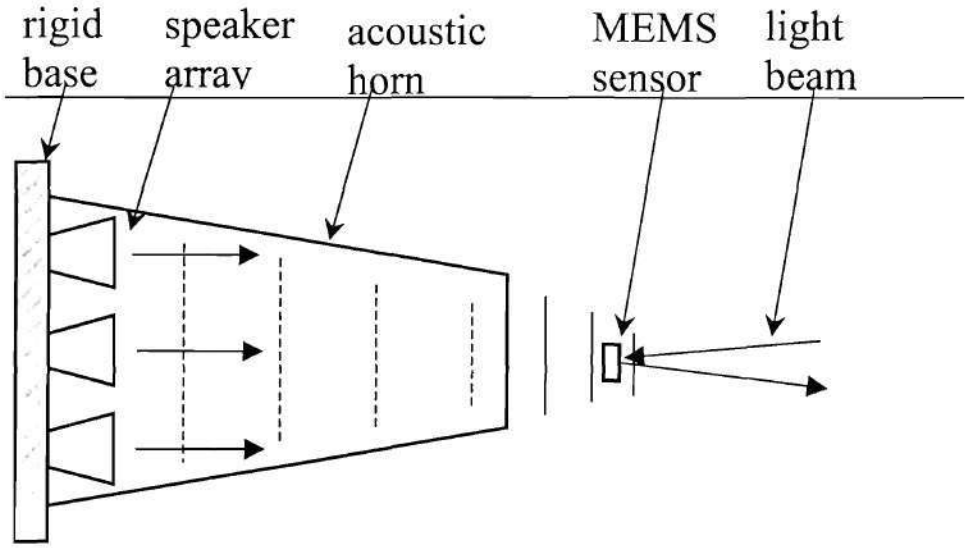

Figure 13. Schematic diagram of the dynamic pressure sensor testbed.

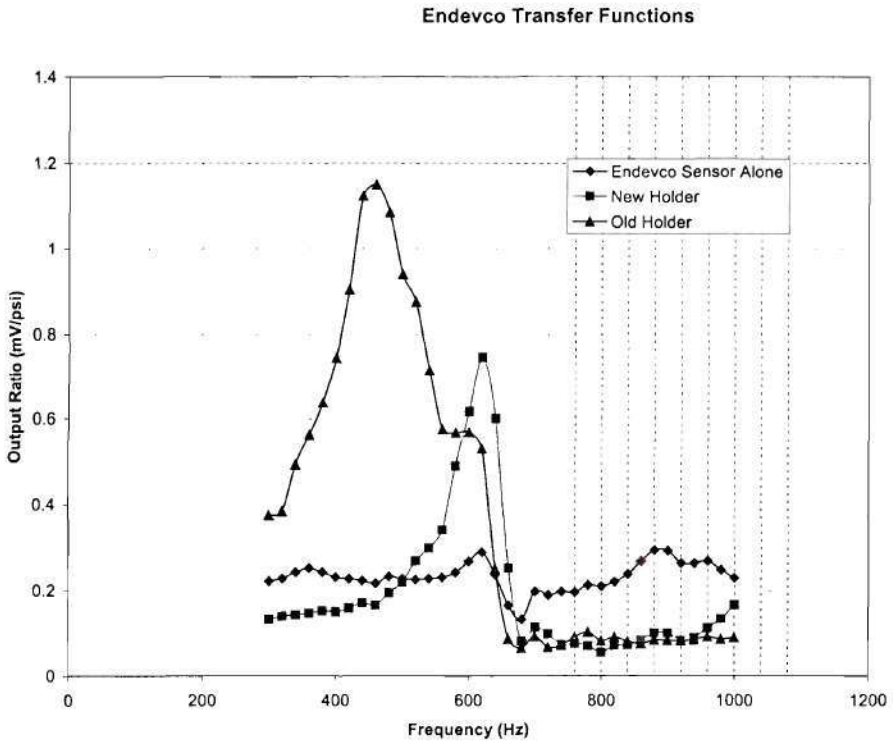

Figure 14. Transfer functions of different holders used in conjunction with Endevco pressure sensor.

Accomplishments to Date: Developed an acoustic calibration procedure for commercial Endevco sensor (the sensor currently used by GEPS), including a transfer function to remove sensor holder's response.

Continuing Work:
Extended for six months under a project titled **Dynamic Pressure Measurements.**

Objective of Dynamic Pressure Measurements Project: The major objective of this project is to design, develop and build a high pressure (static and dynamic) and high-temperature testing facility to calibrate the performance of acoustic sensors for condition monitoring of gas turbine engine components. This dynamic pressure testing facility will then be used to develop a benchmark calibration procedure for acoustic sensors and to develop transfer functions to characterize the effect of sensor mounts. This work will develop a systematic calibration procedure that identifies sources of noise (and their elimination) and improved data acquisition, including signal processing. The final portion of this project will complete optimization and characterization (including survivability/production issues) of the high temperature version of our MEMS sensor.